Program #DE-FC26-04NT42272

Final report on Novel Materials for High Efficiency White Phosphorescent OLED.

October 31, 2008

Submitted by Mark Thompson, University of Southern California (PI)

coPIs: Stephen Forrest, University of Michigan and Brian D'Andrade, Universal Display Corporation.

Our program was a materials intensive one, based on preparing new materials for phosphorescent based white organic LEDs (WOLEDs). Each of our principal projects are summarized below and detailed in the attached published papers.

Year 1:

The milestones proposed for year one are given below. The most important milestone on the list is number 3, achieving a significant advance in white OLED efficiency. This milestone was achieved in two different device architectures (descried in more detail below and in the attached presentation). In one device we used a combination of fluorescent and phosphorescent dopants, leading to external efficiencies of 25% and 36 lum/W, based on device performance in an illumination fixture. These devices gave CIE coordinates between 0.35,0.40 and 0.40,0.40, with CRI values ranging from 75 to 85. We have also prepared high efficiency WOLEDs with devices in a stacked architecture, utilizing red, green and blue phosphorescent dopants (the blue dopant was developed as part of this program). The stacked OLED (SOLED) gave illumination fixture efficiencies of 42% and 49 lum/W. This device gave similar CIE and CRI values to those of the fl/ph OLED described above. The two devices prepared and tested in the first year of this program represent not only completely new approaches to achieving high efficiency white electroluminescence in OLEDs, but also break the previous world's records for WOLED efficiencies by a substantial margin. It is also important to note that there is ample room to improve the efficiencies of these devices further.

Year 1	
Milestone 1	Prepare energy graded hole and electron injectors
Milestone 2	Deep blue electrophosphorescent OLED η_{ext} > 13%
Milestone 3	White OLED with triple doped structure, external efficiency > 14% and > 40 lm/W
Milestone 4	Wide gap host materials in deep blue OLEDs.
Milestone 5	Prepare broadband phosphors, and OLEDs

Milestone 1: The first milestone (prepare energy graded hole and electron injectors) is not an important one to focus our attention on without the successful completion of milestone 2. With that logic in mind we did not work toward accomplishing milestone 1 in the first year of the program, but focused on milestone 2 first.

Milestone 2: While we have successfully prepared deep blue phosphorescent dopants, consisting of Ir based organometallic complexes, with high luminance efficiencies (> 75% PL efficiency in the solid state), we have not been successful in incorporating these new materials into high efficiency blue OLEDs. We have achieved efficiencies of 6%, but not the targeted values of > 13%. Since the luminance efficiencies for the new blue dopants we have developed in this program are very high, our current analysis is that we need to focus on new materials and device architectures, designed to give efficient electrophosphoresce from the new families of blue dopants we have generated. The particular problem that needs to be addressed is that they new dopants have readily oxidized HOMOs and LUMO energies

that make them very difficult to reduce. Our prior blue phosphors were difficult to oxdize and easy to reduce.

Even though we did not meet this milestone directly, we did develop new blue emissive materials, one of which was used in the high efficiency SOLED structure. This device could not have been fabricated with the blue phosphors that existed prior to this program. Thus, while we did not meet this milestone explicitly, we did develop new blue phosphors that enabled the completion of milestone 3, which was the goal of this milestone in the end. We will carry on our work with new blue phosphors, with an aim to achieving high EL efficiency for the new blue materials we have developed.

Milestone 3: This milestone was achieved in two different device architectures (descried in more detail below and in the attached presentation). In one device we used a combination of fluorescent and phosphorescent dopants, leading to external efficiencies of 25% and 36 lum/W, both based on device performance in an illumination fixture. These devices gave CIE coordinates between 0.35,0.40 and 0.39,0.45, with CRI values ranging from 75 to 85. We have also prepared high efficiency WOLEDs with devices in a stacked architecture, utilizing red, green and blue phosphorescent dopants (developed as part of this program). The stacked OLED (SOLED) gave illumination fixture efficiencies of 42% and 49 lum/W. This device gave similar CIE and CRI values to those of the fl/ph OLED described above. The two devices prepared and tested in the furst year of this program represent not only completely new approaches to achieving high efficiency white electroluminescence in OLEDs, but also break the previous world's records for WOLED efficiencies by a substantial margin.

Milestone 4 Two new families of UGH material were prepared and are currently under evaluation.

Milestone 5: Two different materials have been prepared as broadband emitters and are being evaluated in OLEDs.

SOLED WOLED devices: We have demonstrated high-efficiency, stacked organic white light-emitting devices (SOLEDs) employing the three metallorganic phosphors: *fac*-tris(1-(9', 9' dimethyl-2'-fluorenyl)pyrzaolato, N, C2) iridium (III), *fac*-tris(2-phenylpyridine) iridium(III), and iridium(III) bis(2-phenyl quinolyl-N,C2') for blue-green, green and red emission, respectively. A transparent, thermally evaporated 10-nm-thick MoO_3 film interposed between two adjacent electrophosphorescent elements efficiently injects charge into the stacked elements when contacting a Li-doped electron transport layer. The use of MoO_3 along with an electron and hole blocked dual section emissive layer yields maximum external and power efficiencies for a 2-element SOLED (2-SOLED) of η_{ext}, = 24.7±1.9% and η_p = 28.9±2.2 lm/W. The external efficiency scales approximately linearly with the number of independent emissive elements in the stack. Hence, for a 3- SOLED, a maximum η_{ext} = 34.9±2.2 % and η_p = 22.7±1.4 lm/W are obtained, with CIE chromaticity coordinates of (x=0.35, y=0.44). Collection of the waveguided light, accomplished in a simple illumination fixture, increases the external efficiencies by a factor of 1.7. These illumination fixture values are given in the table below.

Combined fluorescent/phosphorescent WOLED: The most efficient WOLEDs reported thus far are based solely on combinations of red, green and blue phosphorescent emitters, allowing for the possibility of 100% internal quantum efficiency (IQE) due to the utilization of both singlet and triplet molecular excited states, or excitons. In the new design devlped as part of our SSL program, we introduce a new principle that allows for the potential of unity IQE with the substitution of a fluorescent material in place of a phosphor for the blue emissive dopant. In this device, triplet diffusion in the conductive host is followed by Dexter exchange to directly excite the green and red phosphors, while the blue fluorescent dopant harvests, in principle, 100% of the singlets via Förster energy transfer. In addition to high quantum efficiency, this scheme allows for an increase in power efficiency of roughly 20% compared with a device that relies solely on electrophosphorence since the exchange energy loss of the blue fluorophore is eliminated. Using a blue fluorophore and green and red phosphrs that have been discussed extensively in the literature, we demonstrate a fluorescent/phosphorescent WOLED with a total external quantum efficiency of (17.0 ± 0.5)% at (1.3 ± 0.5) mA/cm^2, a color rendering index of CRI = 85 and a total power efficiency of 26.9 ± 0.5 lm/W. Using proprietary materials in place of the public domain materials, we have achieved WOLED efficiencies roughly 50% greater, giving values of 25% and 36 lum/W, in an illumination fixture.

Table: SOLED device performance

Device: structure [1]	max η_{ext} (total η_{ext}) [2] (%)	max η_p (total η_p) [2] (lm/W)	max efficiency (cd/A)	voltage at J=10	CIE (x,y) at J=10	Color rendering index
1-SOLED : EL^a	13.6±1.2 (23.1±2.0)	28.9±2.5 (49.1±4.3)	34.9±3.1	9.2	(0.37, 0.46)	62
2-SOLED : $EL^a/MoO_3/EL^b$	24.7±1.9 (42.0±3.2)	28.9±2.2 (49.1±3.7)	66.6±5.0	18.0	(0.39, 0.45)	64
3-SOLED : $EL^a/MoO_3/EL^c/MoO_3/EL^c$	34.9±2.2 (59.3±3.7)	22.7±1.4 (38.6±2.4)	77.0±5.0	24.1	(0.35, 0.44)	66

EL element consists of [NPD (variable thickness) / Irppz (10nm) / 10% Flzlr : mCP (20nm) / 10% PQIr : 3% Ir(ppy)$_3$: CBP (5nm) / Bphen (20nm) / Bphen : Li (1: 1 molar ratio) (20nm)].

NPD thickness in each EL element is EL^a: NPD (40nm), EL^b: NPD (100nm) and EL^c: NPD (60nm).

1) The anode and the cathode for the devices are ITO (150nm) and Al (50nm), respectively.

2) The total efficiency is including light waveguided in the glass substrate and the contact layers. This is the value that would be obtained in an illumination fixture.

data

Year 2:

The milestones proposed for year two are given below. We have achieved each of these milestones to the extent possible and discuss each briefly bellow.

1	Prepare and test shallow HOMO blue phosphors with reducible ancillary ligand
2	• Investigate new materials and device architectures for shallow HOMO blue emitters, new and existing phosphors, target EQE > 10% for non-fluorinated blue emitters • Use new materials and architectures developed above for SOLED and triple doped WOLED, target CRI > 80 and an efficiency > 50 lm/W at 500 cd/m2
3	Couple blue phosphorescent dopant and broadband emitter to achieve efficient two component white, efficiency > 30 lum/W, at 500 cd/m2 or above
4	• Continue architecture development for fluorescent/phosphorescent WOLED, new materials in new structures, designed to optimize process • Make blue fluorescent dopants with small singlet-triplet gap (triplet transfer to host) • Target efficiency > 25 lum/W, CRI > 80, at 500 cd/m2 or above
5	Demonstrate combinatorial system for OLED optimization
6	White OLED with efficiency > 20 lm/W and lifetime > 3,000 hour

Milestone 1: The first milestone (prepare and test shallow HOMO dopants with reducible ancillary ligands) was performed. BWe have found a number of blue emissive dopants which have very high PL efficiencies, but do not generally lead to high EL efficiencies. One common trait among these new blue emitters is that their HOMO levels are markedly above those of the blue phosphors that have been investigated previously. These dopants also have LUMO levels substantially above those of conventional blue phosphors. Our hypothesis is that these dopants are not readily reduced and thus do not efficiently trap electrons in the OLED. This hinders hole-electron recombination at the dopant, limiting device efficiency. Our goal was to take blue phosphorescent dopants with high PL efficiency and add a reducible ancillary ligand, to aid in recombination. IN this type of complex, we theorized that the hole and electron can be trapped on different parts of the molecule and then recombine intramolecularly. We prepared dopants with reducible ancillary ligands, showing accessible oxidation and reduction waves in their electrochemistry. Unfortunately, we found that this led to very low luminance efficiencies for the phosphors. We believe that this was the result of the formation of an internal charge transfer interaction,

which ultimately quenched dopant emission. Thus, the conclusion is that this approach can not be used to achieve higher EL efficiency.

Milestone 2: With our results form the first milestone, we did not progress to milestone 2. This milestone requires the use of a higher efficiency blue phosphor.

Milestone 3: Our first system to examine were dimethylamine derivative. Our preliminary results suggested that these complexes would give broad emission lines when doped into OLED materials. The first complex we prepared was $(ppz)_2Ir(ppy\text{-}NMe_2)$, which gave only red emission in all matrices examined. We then prepared the Pt analog, $(Me_2N\text{-}ppy)Pt(acac)$, which was used to generate our preliminary photophysical data. This complex also gave us only red emission in a range of OLED host materials. After this we chose to move onto to another system. We discovered that binuclear Pt complexes can be used to form broad band emitting materials. We have prepared several different complexes of this type and were evaluated in single dopant OLEDs. We observed both broad emission lines and high device efficiencies. Without new efficient blue phosphors in hand it did not make sense to incorporate these materials into our multiply doped architecture. These materials will be doped into multilayer and fluorescent/phosphorescent structures in the future.

Milestone 4 We focused a significant fraction of our attention this year on the development of the fluorescent/phosphorescent device.

In one of our projects we prepared and studied fluorescent dopants with small singlet-triplet energy gaps. The goal here was to prepare a dopant that would capture singlets from the host material, but not trap triplets in the same matrix One of the families of fluorescent dopants that were examined was built around an indolocarbazole core. These materials have a small singlet-triplet gap (see the spectra shown below, the gap is roughly 0.4 eV). The triplet energy of this material is suitable for doping into CBP and is expected to transfer to the CBP host matrix by endothermic energy transfer. The excitation spectrum matches the CBP fluorescence band very well, and as such we expect efficient Forster energy transfer. Our initial device work with FD-TIC, in a CBP based OLED was disappointing. The peak efficiency was only 1.7 %. We believe that this is due to dopant aggregation in the device and are working now to make bulky analogs that will not show the same level of aggregation and quenching. We have examined the photophysics of these dopants and estimate that their luminance efficiency in the solid state is roughly 0.6. While this value is good, we hope to be able to increase this further in our future studies.

In addition to new dopant approaches, we have examined two SOLED structures for achieving high efficiency from fluorescent/phosphorescent OLEDs. The first structure we examined involved stacking the same devices structures that we have used previously on the hybrid device. We compared 1, 2 and 3 devices in a stack, separated by a MoO_3 charge injecting layer. The stacked approach gives a high external quantum efficiency, and improved luminance efficiency. Using this approach we achieved an efficiency of 22 lum/W at 1000 cd/m^2. Lifetime studies of this device are underway. We also examined a stacked device that utilized phosphor sensitized fluorescence to achieve red emission. In this device the blue light comes form a fluorescent dopant, green form a phosphor and red from a second fluorescent dopant, which is pumped by the green phosphor. This approach is a very powerful one in that we can easily tune the choice of dopant materials to achieve a broad range of bleu and red emission colors. This also limits the number of phosphors required in the device to one, rather than 2. Our initial device work with this structure has led to device efficiencies over 20 lum/W at 1000 cd/m^2. We are continuing to work with this structure and optimize performance.

Milestone 5: We have refined and used our combinatorial system to optimize the structure for white emitting SOLEDs.

Milestone 6: We have made excellent progress on our fl/ph hybrid devices, and have used these devices to meet this milestone. We have now met our lifetime milestone for year two of this project, as shown below. Our Year two milestone is: White OLED with efficiency > 20 lm/W and lifetime > 3,000 hour at 800 cd/m^2. The device prepared in our program had an efficiency of roughly 25 lum/W at 800 cd/m^2 and gave a lifetime of > 4000 hours. The details of this device and the lifetime data are given in the August monthly report.

Year 3:

The year 3 milestones for our program were very aggressive in terms of device efficiency and lifetime. In order to meet these goals we attacked the problem on several fronts.

Blue Phosphor degradation: We took several approaches to solving this problem. The first involved a detailed photophysical study, in which we illustrated that the nonradiative decay pathways for the majority

of blue phosphors, and Ir based phosphors in general, involves a bond rupture process. This has led us to a proposal for improving blue phosphor stability that involves rigidifying the ligands themselves. This work is detailed in an attached draft of a manuscript. In a separate study we showed that the principal decay route for blue phosphorescent devices involves an annihilation event with an exciton on the dopant and a polaron on the host (see attached paper). While this study did not lead to a clear definition of how to solve the problem it indicated that decreased polaron/exciton interaction would enhance device lifetime, which is being explored at this time.

Fluorescent/phosphorescent WOLEDs: In year 2, we described our lifetimes measurements for the fluorescent/phosphorescent WOLEDs. This device met our lifetime milestone for year 2 of the program, but involved an extrapolation from a data set of only 600 hours of stress. We have extended the testing period to > 2000 hours now and see the same lifetime of > 5000 hours, predicted by our previous limited data set. The lifetime plot is shown below.

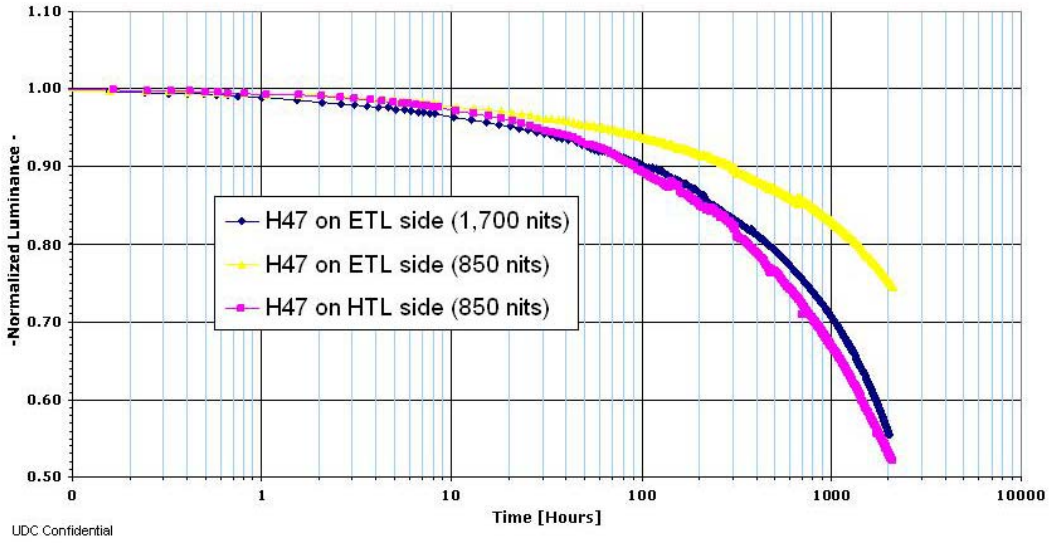

Fluorescent/phosphorescent WOLED lifetimes: In order to improve the lifetime of the fluorescent/phosphorescent devices we need to improve the stability of the n-doped transport layers. The common n-doping technique involves the use alkali metals, which often diffuse out of the ETL and into the emissive region, markedly decreasing the device efficiency. The most common dopants that has been used to n-dope ETL materials are alkali metals, *i.e.* Li, Na, K, Cs. This doping can be accomplished by either codepositing the alkali and ETL material or by depositing the alkali metal onto the ETL material and rely on diffusion of the metal into the ETL. I will use a particular example of n-doping to highlight the problems of using alkali metals as n-type dopants and illustrate how the present invention will solve these problems. One of he most heavily studied systems for n-type doping is the doping of bathocuprione (BCP) with Li. The Li doping leads to a marked increase in conductivity. This system has two problems, however. The Li dopant diffuses over time into the ETL and can eventually diffuse into the emissive layer, leading to marked emission quenching. Thus, a goal of the present invention is to prevent this diffusion process, stabilizing the device while maintaining the benefits of n-doping of the ETL. A second problem seen for Li doping of BCP is that the number of carriers generated in the doping process is a small fraction of the amount of Li that is present in the film. On the order of 1% of the Li leads to free carriers in the film.

The likely reason that diffusion is such a prevalent process in Li doped BCP is that BCP is a reasonably good ligand for Li. The Li ion is certainly coordinated to the BCP (through its two N line pairs) and can readily hop form BCP to BCP. The BCP molecule itself can readily coordinate to the Li ion, so the ion could move through a neutral BCP lattice or it could migrate with the electron from BCP to BCP. The fact that Li doping generates a small number of carriers is related to this coordination. In the

absence of any electric field, the Li ion is most likely coordinated to the reduced BCP. This is in effect a tightly coupled hole-electron pair. In order to generate a free carrier the field must dissociate the pair and force the electron to migrate to an adjacent BCP. The tight binding is a high energy state and breaking out the free charge may require a fairly high field. The present invention seeks to solve both of these problems by adding a Li chelator to the film. Crown ethers and cryptands are very well known to bind strongly to alkali ions. An example of such a compound is shown in the attached paper. Li forms much stronger bonds to oxygen donors than nitrogen, so it is thought that the Li ion formed in the doping process will selectively bind to the crown ether rather than the BCP or BCP anion. The crown ether will effectively insulate the Li cation from the BCP anion, markedly decreasing the hole-electron binding energy and freeing the charge. The crown will also act to stabilize the film toward Li ion diffusion, since the Li can hop form crown to crown, but is not expected to leave the region of the device that is doped with the crown ether. Thus, an entire BCP layer could be doped with the crown or only the part of the layer that is meant to be doped, leaving an undoped BCP region.

The use of a crown ether or cryptand can trap the alkali ion, and prevent its diffusion out of the ETL. We have examined the sue of crown ethers previously (see attached paper) and found that they are too volatile to use in our vacuum deposition systems. Switching to a cryptand leads to lower volatility, but they could not be sued in the UDC systems. We have recently found that coordinating the cryptand to a metal salt will give a low enough volatility to make them useful in a conventional deposition system. The slat stabilized crytpand will be evaluated at UDC for its effect on device lifetime soon. Device data on this cryptand is given below. We are currently exploring the use of these amteirals in WOLEDs and how this impacts their lifetime.

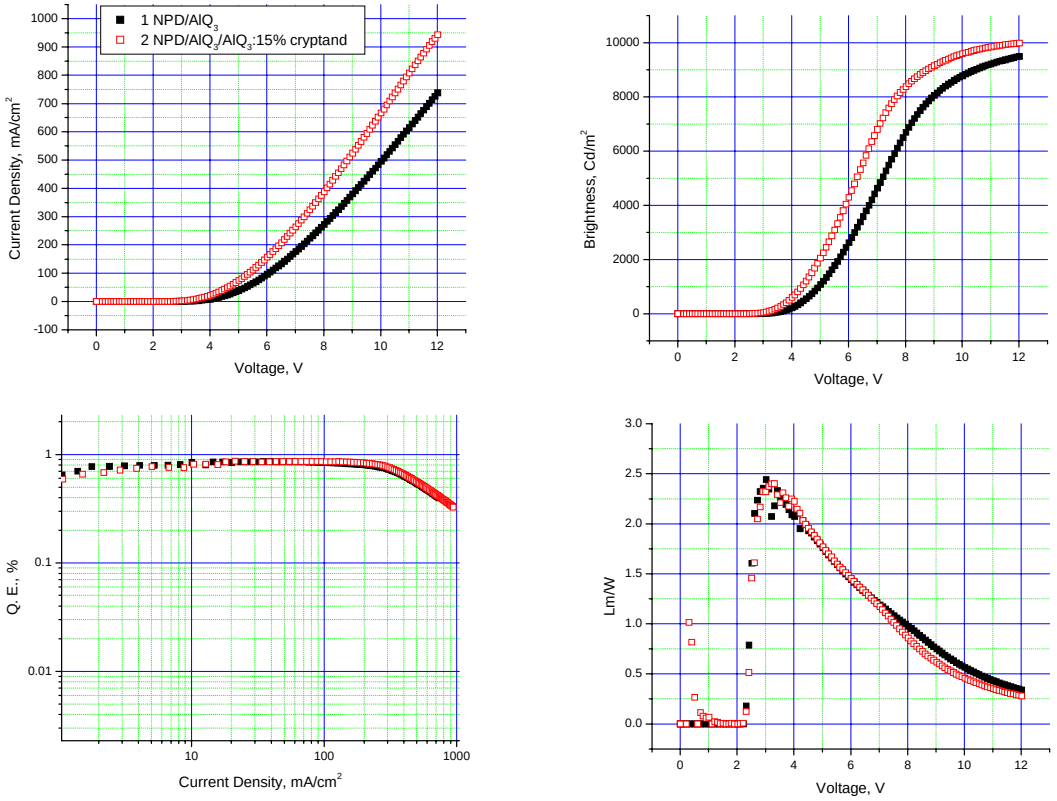

<u>Simple fluorescent/phosphorescent WOLED structure:</u> We are investigating a new approach to improve the performance of our fluorescent/phosphorescent hybrid WOLED, previous device structure shown in Fig. 1(a). The proposed advanced structure is shown in Fig. 1(b). In this device, all excitons are formed on host molecules near Host/BCP interface, different from the two recombination interfaces in previous structure. Singlets are transferred to the fluorescence dopant close to recombination zone, while triplets diffuse out to phosphor-doped region which is separated by a spacer layer and get harvested there. The key points to success are having the HOMO level of the host above those of dopants and the triplet energy of host molecules lower than that of the fluorescence dopant so that charge trapping on both dopants and triplet

excitons trapping on the fluorescence dopant can be avoided.

Based on the considerations mentioned above, S_1/T_1 state of the host need to be separated wide enough to bracket the ones of fluorophor dopant. A series of host and fluorophor molecules have been synthesized and studied. Some of triaryldiamines are known for their shallow HOMO and good hole conductivity. All the host molecules (**1, 2, 3**) here contain this substructure. Their oxidation potentials are 0.15eV to 0.25eV versus Fe/Fe^+ suggesting a shallower HOMO than most of widely-used hosts and dopants nowadays. They are made by coupling diarylamines and dibromo-derivatives of core moiety together, with the presence of sodium *tert*-butoxide, trace amount of palladium(II) acetate and tri-*tert*-butylphosphine. **4**, as a dopant, is designed to have a narrow S_1/T_1 gap, which relaxes the criteria on the S_1/T_1 gap for the host. Their structure and photoluminescence data in solid state are listed in Fig. 2 and Table. 1. As shown, a good host/fluorescence dopant combination has not been found yet. We are trying more variations of triaryldiamine by using different aryl groups in order to widen the S_1/T_1 state gap while still keep HOMO in the same range.

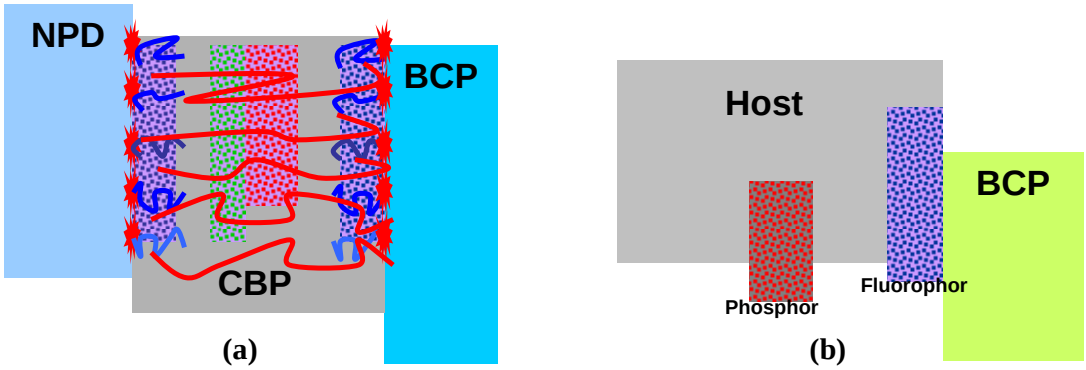

Fig. 1. (a) structure used in previous work. (b) proposed improved structure.

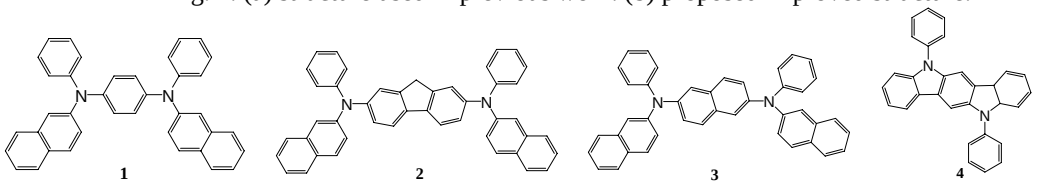

Fig. 2. Structures of synthesized molecules

Table. 1 Photoluminescence data of molecules

	1	**2**	**3**	**4**
S_1	440nm	435nm	440nm	420nm
T_1	540nm	535nm	550nm	480nm

However, some devices with similar structure have optimistic results. Fig. 3 shows the external quantum efficiency, brightness and J-V characteristics for ITO/**1** (20nm)/**1**:7%PQIr (20nm)/**1** (10nm)/mCP or CBP or **1**:5% **4** (20nm)/BCP (40nm)/LiF (1nm)/Al (120nm) OLEDs. From Table 1, it is clear that the energy of singlet excitons formed on **1** can not be transferred to dopant, **4**. As a result, the device using **1** as the only host has lower quantum efficiency and brightness. On the other hand, this device has better conductivity indicating **1** transporting charges well. The other two devices having mCP and CBP as the host for fluorophor, **4**, have demonstrated the concept that the triplet excitons can be generated and harvested at different regions due to their long lifetime. This concept is better presented in this structure than the one in Fig. 1(a), because it basically rules out the probability of excitons directly being formed on phosphorescence dopant. With part of idea realized, mCP and CBP's deep HOMO and high triplet energy undermined the rest of plan by losing triplet excitons in fluorphor-doped region. Some excitons might have formed on fluorophor, **4**. Those triplets are confined by high-energy host molecules and decay radiationlessly. Fluorophor dopant itself might serve as triplet traps annihilating high-energy triplets nearby.

The device with proposed structure, i.e. ITO/**1** (20nm)/**1**:7% PQIr (10nm)/**1** (10nm)/**1**:5% **2** (10nm)/mCP

(10nm)/BCP (40nm)/LiF (1nm)/Al (120nm), gave off little PQIr emission and low efficiency. Thin film study reassures it is not that PQIr is quenched by **1.** Two sets of devices were made in aim to find out what the reason might be.

The first set of devices has structure, ITO/**1** (30-X nm)/ **1**:5% **2** (10nm)/**1** (X nm)/mCP (10nm)/BCP (40nm)/LiF (1nm)/Al (120nm). X equals to 0, 5 and 10nm for Device 1, 2 and 3. In these devices, with the thickness kept unchanged, fluorophor-doped layer was moved away from **1**/mCP interface. The electroluminescence, external quantum efficiency, brightness and *J-V* curve are shown in Fig. 1.

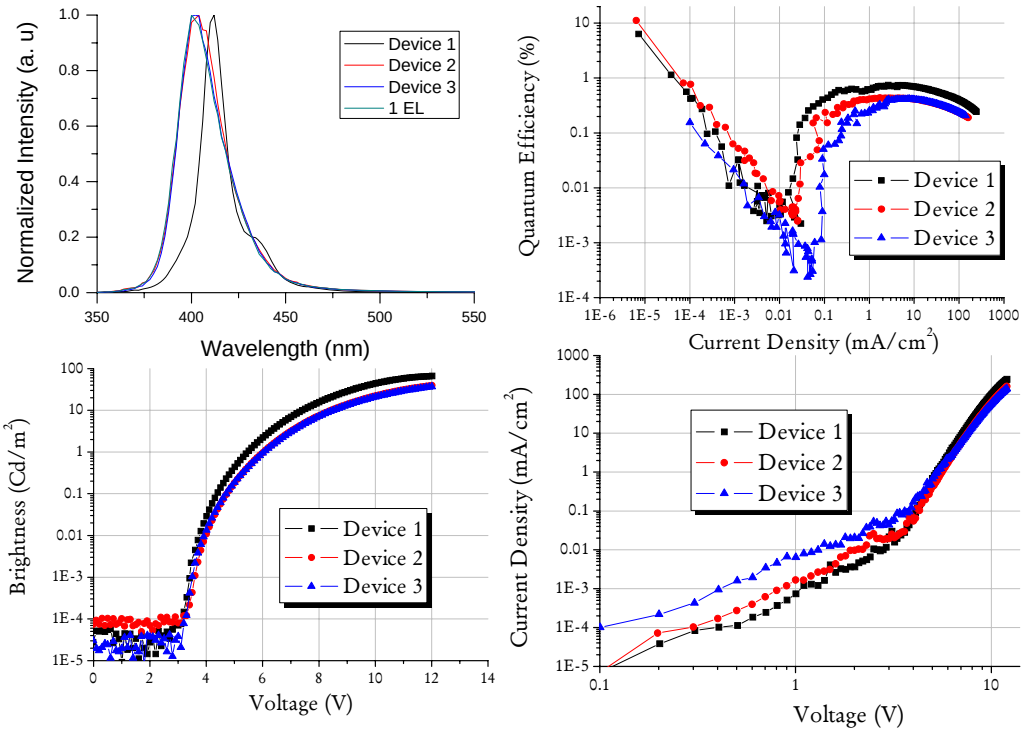

Fig. 1. Electroluminescence at 9V (upper left), external quantum efficiency (upper right), brightness (bottom left) and *J-V* curve (bottom right) of first set of devices

Figure 1 shows only device 1, in which **2** was doped up to **1**/mCP interface, has the emission of dopant, while the other two devices emits just like a thin film of **1.** This reveals that the recombination zone is, as expected, very close to **1**/mCP interface. 5nm away from the interface is far enough for **2** molecules to receive energy from singlet excitons formed in recombination zone. Device 2 and 3 have same efficiency and brightness curve proves the irrelevance of the distance from doped layer to **1**/mCP interface once they are separated up to certain extent. All three *J-V* curves possess similar characteristics, which confirmed **1** molecules as the role player of charge transportation.

With this known, the second set of devices were made with structure ITO/**1** (30-X nm)/ **1**:7% PQIr (10nm)/**1** (X nm)/mCP (10nm)/BCP (40nm)/LiF (1nm)/Al (120nm). The only difference here is that the fluorophor dopant was replaced by a phosphor one. Both dopants have deeper HOMO than **1,** the host**.** Given all devices having the same thickness, this change of dopant should not affect *J-V* characteristics. The data is shown in Fig. 2.

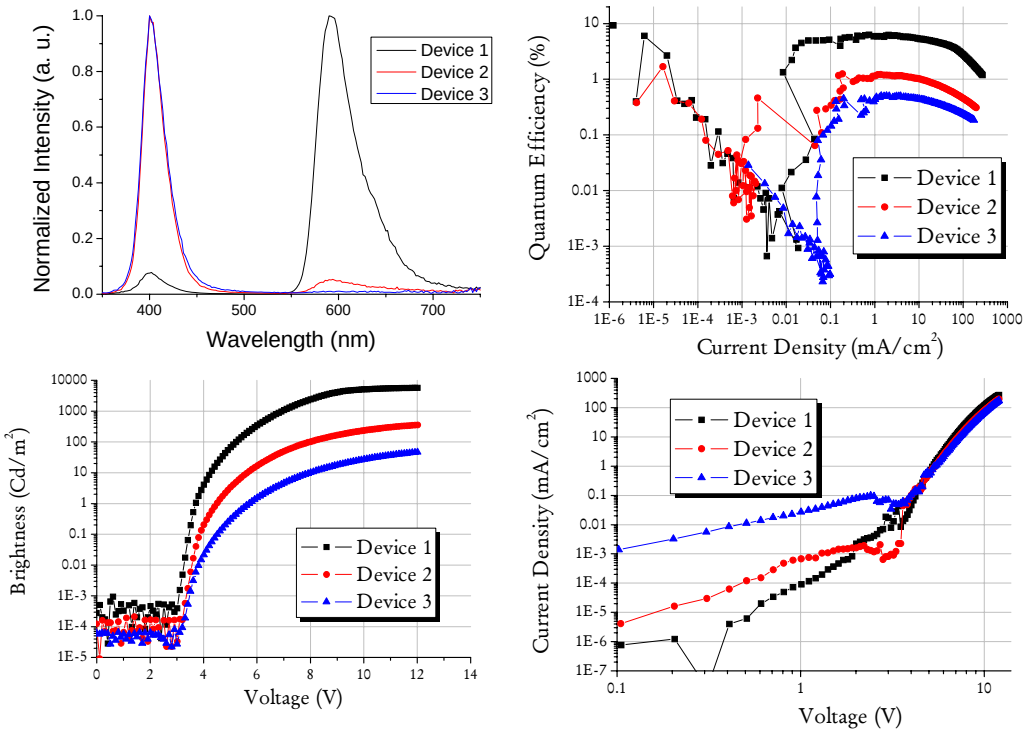

Fig. 2. Electroluminescence at 9V (upper left), external quantum efficiency (upper right), brightness (bottom left) and *J-V* curve (bottom right) of second set of devices

Device 1 is a phosphorescence device and recombination happened in adjacent area so that excitons were captured by phosphors with lower energy. In Device 2, the small portion of PQIr emission has to be from excitons that made their way out of recombination zone, because there is no recombination happens directly on dopant molecules in this case and also this structure is proven by previous case that dopant layer is out of the radius of Foster energy transfer, which rules out the possibility PQIr harvest some singlet excitons nearby. Device 3 is just like Device 2 and 3 of first set. Dopant does not contribute since all the channels for energy transfer are shut down due to the distance.

These two sets of devices explicitly demonstrated the exciton diffusion. They also found out matrix of **1** is very resistant to exciton diffusion. The explanation for that is the poor overlapping between molecules. **1** was designed to have less overlapping than molecules without t-butyl groups hoping to minimize the red shift of emission in solution to solid state so that it has enough high energy to host **2**. However new problem stemmed out. New host/fluorescence dopant system will be studied in following work.

Broadband emitters: We have examined a number of Cu containing phosphors. These materials have been reported to give broad line emission. We have not found any useful materials. The emission lines we have observed are broad, but very weak. We have also found that the materials are thermally sensitive.

We are approaching this issue from another side as well. Our phosphors exist in two conformations: facial and meridianal. The meridianal isomer gives a much broader line than the facial derivative, due to its lower symmetry. We have begun the investigations of a representative member of this family. The meridianal $Ir(bzq)_3$ complex has been made and the emission spectrum is in fact very broad (see below). The doped thin films samples (red trace) efficiently cover half of the visible spectrum. We are scaling this material up for device studies now.

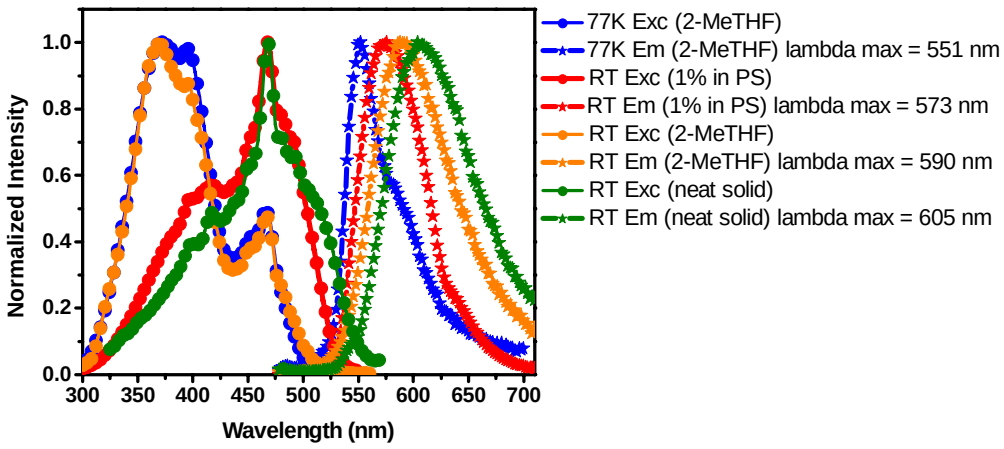

Monochromatis mer-Ir(bzq)$_3$-doped CBP devices have been fabricated with a device structure of ITO/ NPD(400Å)/ mer-Ir(bzq)$_3$:CBP (8%, 250 Å)/ BCP(400 Å)/ LiF(10 Å)/ Al (1100 Å). This monochrome device turns on at a low voltage of 2-3V and the electroluminescence comes from the broadband emitter, mer-Ir(bzq)$_3$ with a maximum external quantum efficiency of 7.43% and a maximum brightness of about 10,000 Cd/m^2 with CIE coordinates: x= 0.33, y= 0.63 (**Figure 2**). The analogous mCP devices were also fabricated, but they do not perform as well as the mer-Ir(bzq)$_3$-doped CBP devices due to their low external quantum efficiencies and high current shortages.

To achieve white electroluminescent OLEDs, we demonstrated two different approaches. One is to use two phosphorescent dopants in one device structure such as the broadband phosphorescent emitter, mer-Ir(bzq)$_3$, with the efficient blue-green phosphor (flzIr; CIE, x= 0.16, y= 0.50). The phosphorescent molecules harness the triplet excitons constituting 75% of the bound electron-hole pairs that form during charge injection; the all-phosphor-doped devices have the potential for 100% internal quantum efficiency. One of the phosphors-doped WOLED device structures consisting of ITO/ NPD(400Å)/ flzIr: mCP (8%, 100 Å)/ mer-Ir(bzq)$_3$:CBP (8%, 100 Å)/ BCP(400 Å)/ LiF(10 Å)/ Al (800 Å) turns on at a low voltage of 2-3V and the electroluminescence comes from both phosphorescent emitters, flzIr and mer-Ir(bzq)$_3$, with a maximum external quantum efficiency of 11.6% and a maximum brightness of roughly 10,000 Cd/m^2 with CIE coordinates: x= 0.38, y= 0.50. In addition, these flzIr-mer-Ir(bzq)$_3$-doped devices are not voltage-dependent. However, the NPD emission shows more significantly as the voltage increases (**Figure 3**). A good blocking layer such as fac-Ir(ppz)$_3$ can definitely solve this issue without decreasing the device efficiencies. In addition, we also fabricated devices in which mer-Ir(bzq)$_3$-doped layer is sandwiched between two flzIr-doped layers; the device performance is similar to the simple double-doped layers devices except the electroluminescent performance (CIE coordinates: x= 0.47, y= 0.48). The mer-Ir(bzq)$_3$ sandwiched type devices show more broadening effects on the EL, up to 750 nm (**Figure 4**).

The second approach is to introduce a different concept by incorporating blue fluorescent emitter such as DTIC in exchange for a phosphorescent dopant, in combination with the broadband phosphorescent emitter, mer-Ir(bzq)$_3$, to obtain high power efficiency and stable color balance while maintaining the potential for 100% internal quantum efficiency. Energy transfers within this second type of device channel nearly all of the triplet energy onto the phosphorescent dopant, retaining the singlet energy exclusively on the blue fluorescent dopant. Eliminating the exchange energy loss to the blue fluorophore allows for about 20% increased power efficiency compared to a fully phosphorescent device. Devices consisting of ITO/ NPD(400Å)/ DTIC: CBP (8%, 200 Å)/ CBP (50 Å)/ mer-Ir(bzq)$_3$:CBP (8%, 50 Å)/ BCP(400 Å)/ LiF(10 Å)/ Al (1100 Å) were fabricated and they turn on at a low voltage of 2-3 V, giving a maximum external quantum efficiency of about 5% and a maximum brightness of roughly 5,000 Cd/m^2 with CIE coordinates: x= 0.29, y= 0.35. These fluorescent-phosphorescent doped devices are voltage dependent. The mer-Ir(bzq)$_3$-doped layer sandwiched between DTIC-doped layers devices were also demonstrated with a device structure consisting of ITO/ NPD(400Å)/ DTIC: CBP (8%, 100 Å)/ CBP (50 Å)/ mer-Ir(bzq)$_3$:CBP (8%, 50 Å)/ CBP (50 Å)/ DTIC: CBP (8%, 100 Å)/ BCP(400 Å)/ LiF(10 Å)/ Al (1100 Å). The CIE coordinates of these sandwiched devices is: x= 0.52, y= 0.34. The device performances of the sandwiched devices are inferior to the simple double-doped layers devices and are still voltage dependent.

Previously, it has been reported that white OLEDs with a maximum external quantum efficiency of 11.6% and a maximum brightness of roughly 10,000 Cd/m^2 (CIE coordinates: x= 0.38, y= 0.50) could be achieved by incorporating only two phosphorescent emitters: a blue-green phosphor (fac-flzIr) and a yellow-orange phosphor (mer-Ir(bzq)$_3$). Recently, analogous device structures with a carbene analog of fac-flzIr (fac-flimIr) as a blue-green phosphor have been fabricated. Since the emission of fac-flimIr is about 15nm blue-shifted from that of fac-flzIr at 77K and RT (**Figure 2**), it is very tempting to apply this carbene analog of flzIr for the white OLED applications especially to achieve better CIE coordinates.

Just like the monochrome fac-flzIr: mCP device, monochrome fac-flimIr: mCP device also emits from the dopant itself (fac-flimIr) and turns on at a low voltage of 2-3V. As an advantage over flzIr device, flimIr device emits in a bluer region (~466nm). As drawbacks, flimIr: mCP device gives a lower brightness and a lower external quantum efficiency compared to those of flzIr: mCP device (**Figure 3**).

The first fac-flimIr: mer-Ir(bzq)$_3$ devices fabricated consist of ITO/ NPD(400Å)/ 8% fac-flimIr in mCP (150 Å)/ 8% mer-Ir(bzq)$_3$:CBP (100 Å)/ BCP(400 Å)/ LiF(10 Å)/ Al (1000 Å). This device has a maximum external quantum efficiency of about 7% and a maximum brightness of roughly 5,000 Cd/m^2 with CIE coordinates: x= 0.29, y= 0.37 (**Figure 4**). Compared to fac-flzIr: mer-Ir(bzq)$_3$ devices, this device has a lower quantum efficiency and brightness. However, the turn-on voltage is still quite low (2-3V) and the EL still comes from both phosphorescent dopants. This device is voltage-independent and the NPD emission shows more significantly as the voltage increases. A good blocking layer such as fac-Ir(ppz)$_3$ can definitely solve this issue without decreasing the device efficiencies. The CIE coordinates for this fac-flimIr: mer-Ir(bzq)$_3$ device is x=0.29, y=0.37, getting closer to the CIE of RGB White (x=0.30, y=0.30). The CIE coordinates of this fac-flimIr: mer-Ir(bzq)$_3$ has been improved compared to previously reported fac-flzIr: mer-Ir(bzq)$_3$ devices. A change in fac-flimIr: mCP layer thickness can definitely affect the recombination zone. By changing fac-flimIr: mCP layer from 150 Å to 100 Å and leaving the mer-Ir(bzq)$_3$: CBP layer constant, more exciton recombinations happen in mer-Ir(bzq)$_3$:CBP layer (**Figure 4**).

The other project that I would like to discuss in this report is about how well we can adjust the levels of facial and meridional isomers from a single boat by monitoring the EL spectra. 100 mg of fac-Ir(ppy)$_3$ and 100 mg of mer-Ir(ppy)$_3$ were mixed onto the mortar and grinded together using a pestle then were transferred into a single boat. The device efficiency and brightness of the device consisting ITO/ NPD(400Å)/ 7% 50:50 mix fac:mer-Ir(ppy)$_3$ in CBP (250 Å)/ BCP(400 Å)/ LiF(10 Å)/ Al (1000 Å) were about 9% and roughly 10,000 Cd/m^2. The external quantum efficiency and brightness of 50:50 fac-mer mixture of Ir(ppy)$_3$ device are similar to those of 100% fac-Ir(ppy)$_3$ device and 100% mer-Ir(ppy)$_3$ device. Nevertheless, at this point, it is still not clear why the device using 50:50 mixture of pure fac and mer-Ir(ppy)$_3$ as a dopant appear to be not exactly 50:50 mixture sublimed out during the vapor deposition according to its EL spectra (**Figure 5**). It appears that more facial isomer is being sublimed onto the substrate in the chamber. The next thing to do is to try to sublime 50:50 mixed fac- and mer-Ir(ppy)$_3$ using a sublimator and monitor what is actually sublimed out at first by NMR. If there is more than one band, we should check the NMRs of each band and see if the percentage of isomers is consistent in each band. If each band does not have the same percentage mixture of each isomer, it is definitely not a trivial thing to adjust the levels of facial and meridional isomers from a single boat in the chamber.

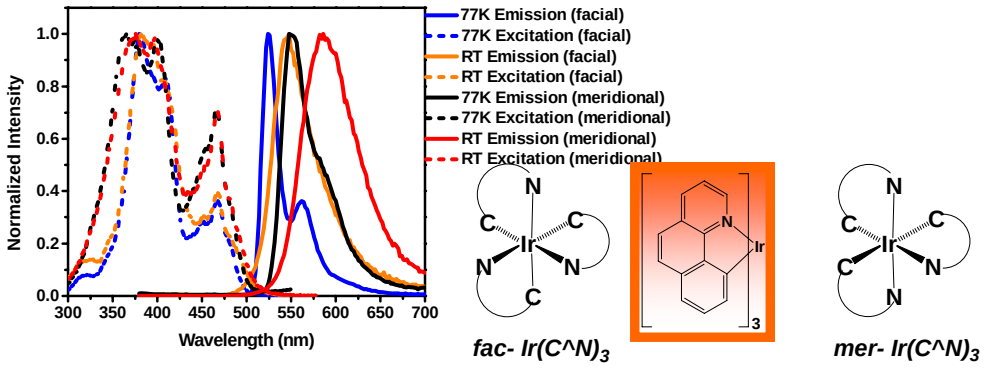

Figure 1. Photophysical Properties of fac-Ir(bzq)$_3$ and mer-Ir(bzq)$_3$

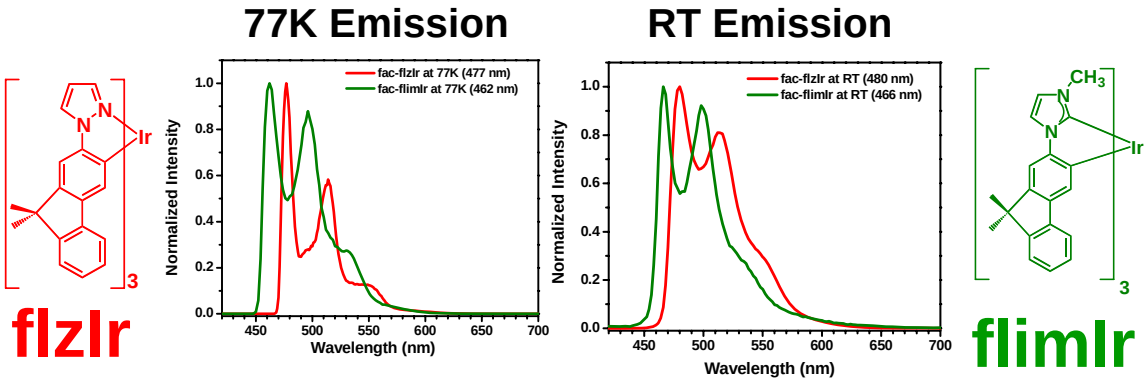

Figure 2. Photophysical Properties of flzIr vs. flimIr in 2-MeTHF

ITO/ NPD (400 Å)/ 8% DOPANT: mCP (250 Å) / BCP (400 Å)/ LiF/ Al

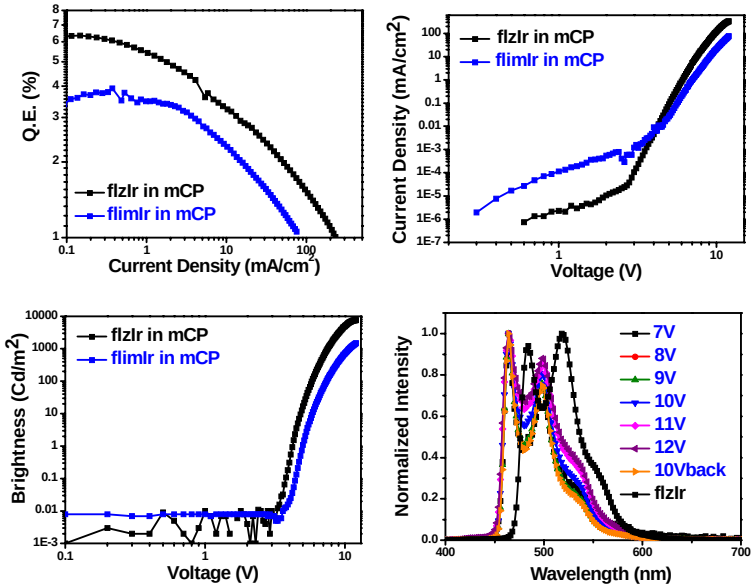

Figure 3. Device Data for Monochrome Device flimIr vs. flzIr in mCP

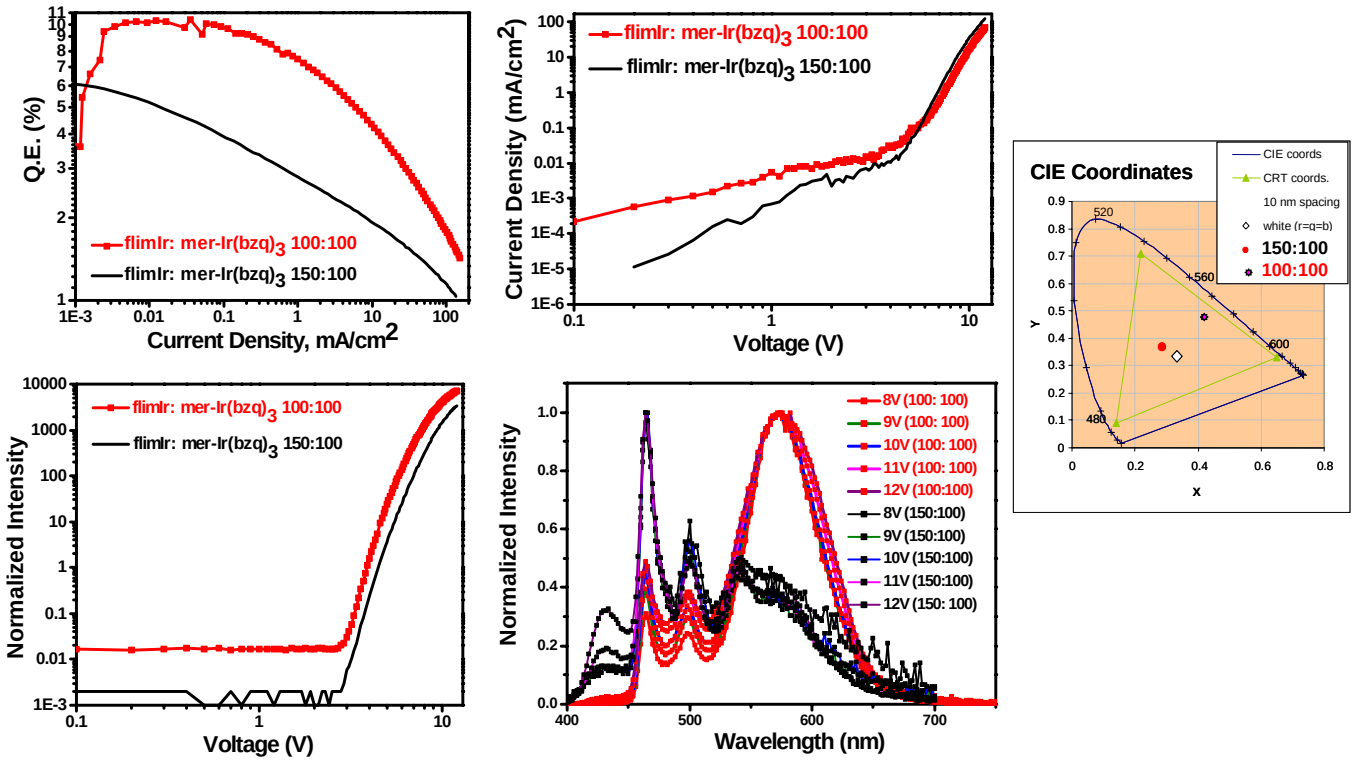

Figure 4. White OLEDs from flimIr: mer-Ir(bzq)$_3$ along with their CIE coordinates

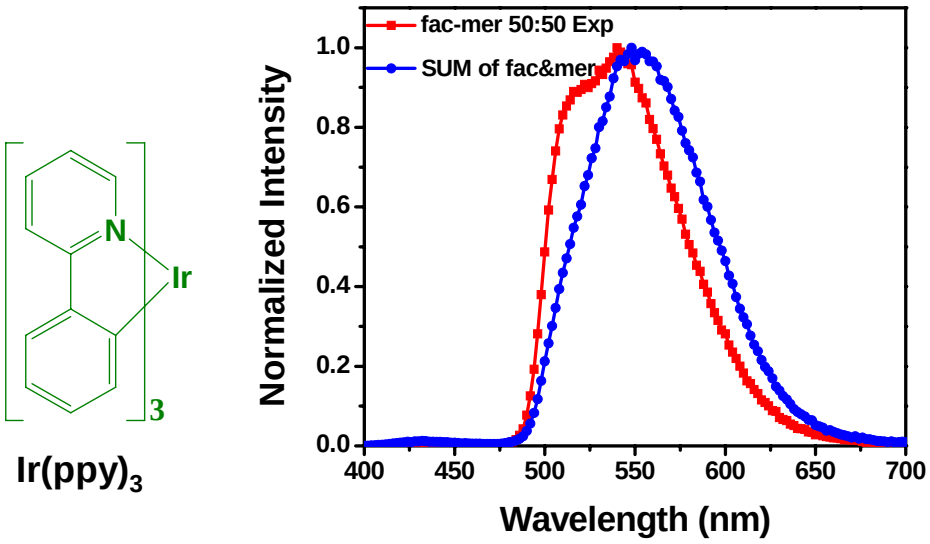

Figure 5. EL Spectra for Expt. vs. Theo. (50:50) fac:mer-Ir(ppy)$_3$

Two component WOLED: We have also investigated the use of two component devices to achieve soft white electroluminescence. The data for one such device is given below. The device structure and materials composition have not been cleared for release yet, but will be included in our next report. This devices gives an efficiency of 33 lm/W at a brightness of 1000 cd/m^2.

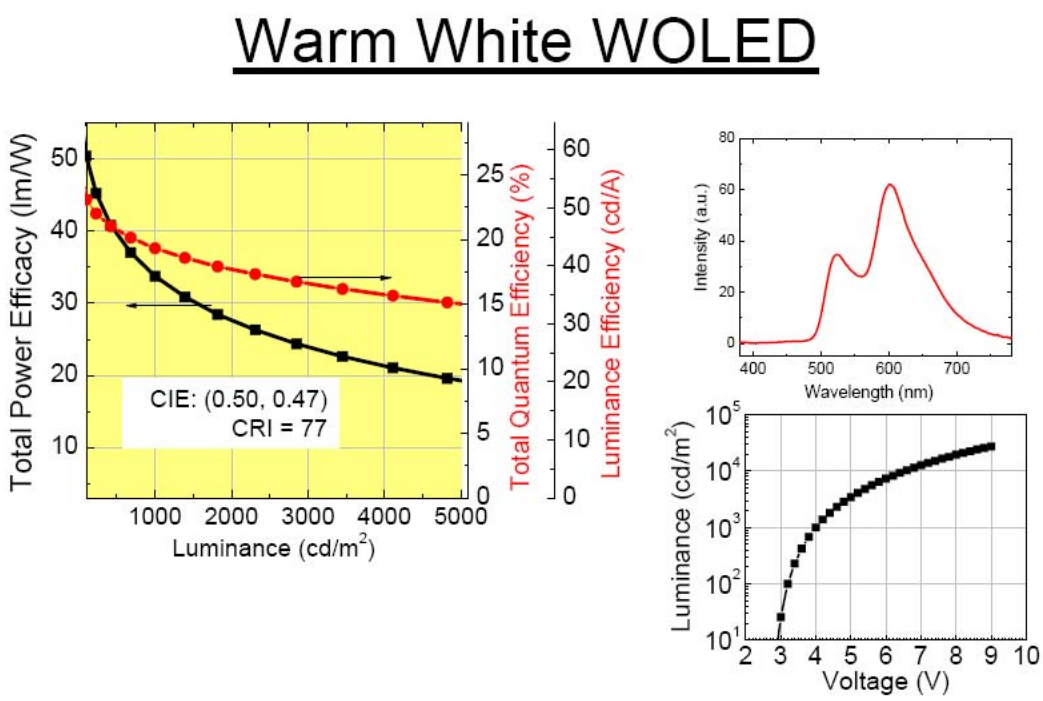

Three Emission-Layer White Organic Light Emitting Devices

In this three emission-layer (EML) white organic light emitting device (WOLED), 3 ambipolar materials with different (small to large) HOMO-LUMO gaps are used as hosts in 3 EMLs, doped with red, green, and blue phosphors respectively. These 3 bipolar layers result in exciton formation in multiple regions, instead of at one interface as in many other WOLED structures. The expansion of the exciton generation region can suppress exciton annihilation effects and let the formed excitons have more chances to radiatively decay through phosphors in all the exciton formation regions, leading to higher efficiencies of this WOLED, even compared to R, G, B mono-color OLEDs.

The multi-EML WOLED is developed from the following 3 mono-color OLED structures: Device 1) NPD 40nm/ MCP 15nm/ 22% FIr6:UGH2 20nm / BCP 40nm /LiF 0.8 nm/ Al 60nm; Device 2) NPD 40nm/ TCTA 10nm/ 10% Irppy: MCP 25nm/ BCP 40nm /LiF 0.8 nm/ Al 60nm; Device 3) NPD 40nm/ 8%PQIr:TCTA 25nm/ BCP 40nm . The maximum external quantum efficiencies (EQE) are 7.2%, 9.6%, 6.4% for Devices 1), 2), and 3), respectively. In Device 1), MCP works as an electron blocking layer (EBL). And in the meanwhile, it has smaller HOMO-LUMO gap compared to the host material UGH2 in the EML. the match-up between the HOMO of MCP and of the blue dopant FIr6 in EML results in efficient hole injection (HIL) to the dopant, which can help enhance efficiency and lower the driving voltage. TCTA functions similarly in these 2 aspects in Device 2). Schematic drawings of

these 3 device structures are in Fig. 1.

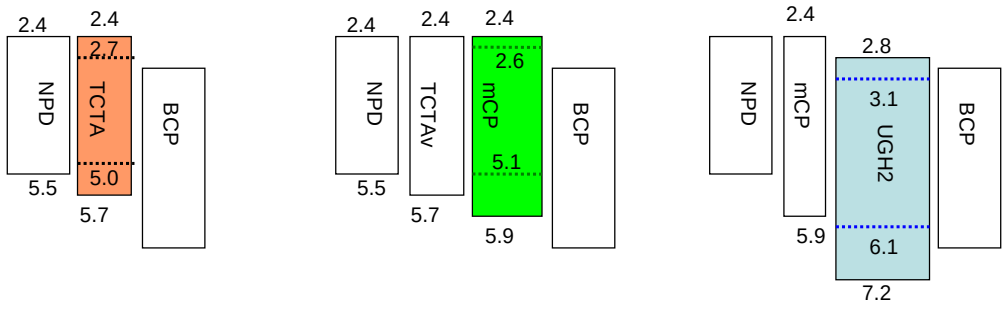

Fig. 1

The 3-EML WOLED structure is schematically illustrated in Fig. 2. In this 3-EML WOLED, we dope the MCP and TCTA layers with $Ir(ppy)_3$ and PQIr respectively. Therefore these 2 layers function as both the EML for longer-wavelength emission and the EBL/HIL to the adjacent shorter-wavelength EML to its right.

Electrons and holes that enter the multi-EML system via bipolar host materials are slowed down, and are likely to recombine in the 3 doped zones of EML rather than highly accumulating at the high barrier of the interfaces. The expanded exciton generation region can depress the exciton annihilation effect due to reduced local density of excitons, and thus lead to higher EQE of 16.6% and PE of 32 lm/W. The efficiency performances are demonstrated in Fig. 3. It is noticeable that the EQE of the 3-EML WOLED is even higher than the mono-color OLEDs discussed above. This confirmed the excitons are better utilized in the multi-exciton-generation-region WOLED.

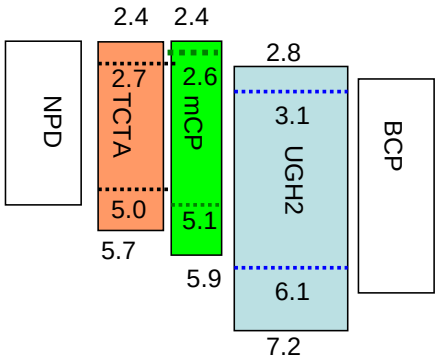

Fig. 2

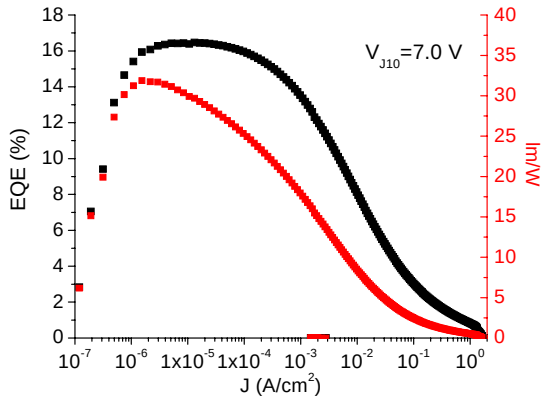

Fig. 3

To better understand the exciton formation region in the 3-EML WOLED, we refer back to the spectra of Device 1). It shows short wavelength emission (Fig. 4(a)), while that of Device 2) does not (Fig. 4(b)). This indicates excitons are mainly formed in MCP and UGH2 layers. In addition, due to the hole barriers existing at TCTA/MCP and MCP/UGH2 interfaces, excitons may also formed at these 2 interfaces.

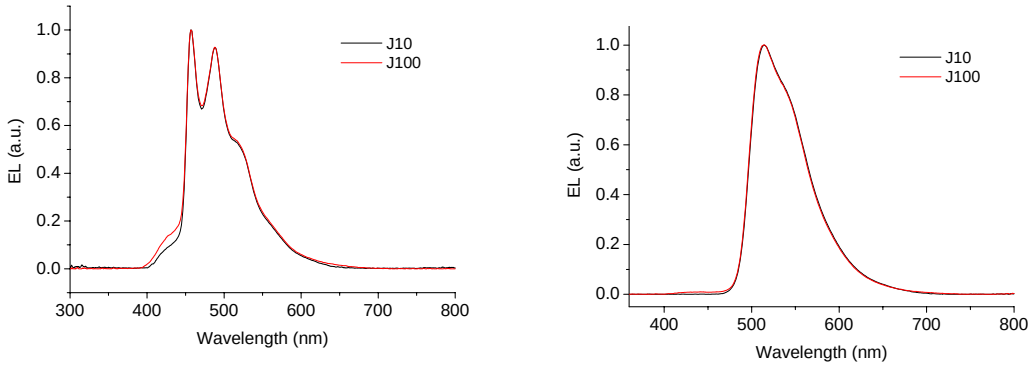

(a) (b)

Fig. 4

The spectra of the 3-EML WOLED are shown in Fig. 5(a). When the current density increases from 1 to 100 mA/cm^2, the CIE coordinates shift from (0.35,0.38) to (0.40,0.39), and the CRI values remain at 80. The interpreted ratio of contribution of red, green, and blue emission in the spectra (Fig. 5(a)) is plotted *vs.* current density in Fig. 5(b). It is shown that red emission gets stronger with current density. This may be because more and more energy transfer occurs between green to red dopants while exciton density becomes higher in $Ir(ppy)_3$ doped region.

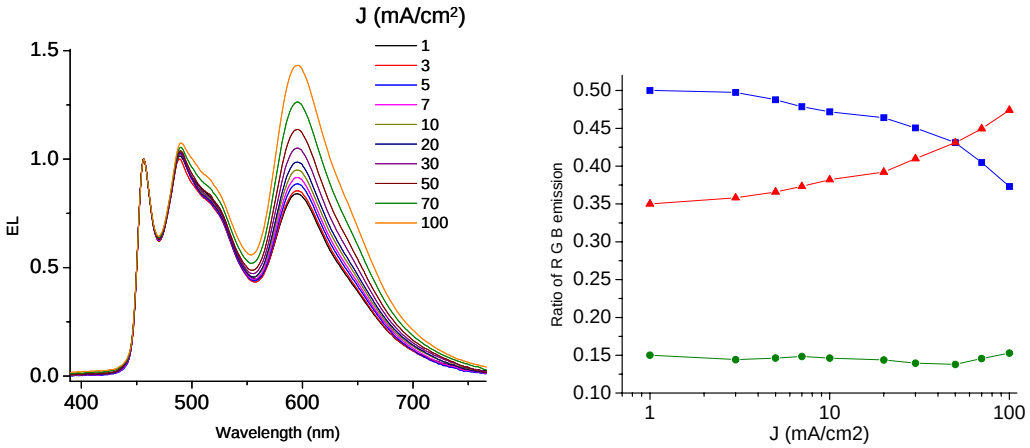

(a) (b)

Fig. 5

In addition, this structure may provide potential advantage of device stability, as the interface between the EML and the HBL is typically a critical issue for long term stability in OLEDs which form excitons at such interface.